Available online at www.sciencedirect.com

ScienceDirect

Procedia CIRP 55 (2016) 188 – 193

www.elsevier.com/locate/procedia

5th CIRP Global Web Conference Research and Innovation for Future Production

Influences of Powder Compaction Constitutive Models on the Finite Element Simulation of Hot Isostatic Pressing

A. M. Abdelhafeez[a,*] , K. E. A. Essa[a]

[a] *Department of Mechanical Engineering, School of Engineering, University of Birmingham, Birmingham B15 2TT, UK*

* Corresponding author. Tel.: +44(0)1214145159; fax: +44(0)1214147484. *E-mail address:* a.m.abdelhafeez@gmail.com; k.e.a.essa@bham.ac.uk

Abstract

Hot isostatic pressing (HIPing) is a promising near net-shape manufacturing technology that can be employed for fabrication of complex parts out of metal powders. Design of tooling/canister that allows net-shape HIPing is still based on expensive experimental try-outs and subsequent iterations to modify the initial canister geometry. An auspicious alternative approach is finite element (FE) simulation. However, the FE results are strongly dependant on the implemented powder metal constitutive model. The current research shed the light on finite element analysis of HIPing process, based on steel 316L powder, using three different constitutive models namely; CAM-Clay, modified Drucker-Prager and modified Drucker-Prager with creep. Comparison with experimentally deformed final geometry and densification history of the HIPed material were carried out. Discrepancies in predicted final geometry dimensions were ranging from 1% to 6.34% compared to experimental trials. Drucker-Prager with creep constitutive model showed the highest accuracy in final geometry predictions with relative error of 1.5~4.8%.

Peer-review under responsibility of the scientific committee of the 5th CIRP Global Web Conference Research and Innovation for Future Production

Keywords: Hot Isostatic pressing; Finite element; Powder compaction; Constitutive model.

1. Introduction

In the HIP process, high temperature (about 70% of the melting point) and high pressure (generally 100-200 MPa) are simultaneously applied to encapsulated powder particles resulting in fully dense components and almost isotropic material properties [1]. The ability to produce near net-shape workpieces (reducing costly machining) has been a major driving force for its commercial advancement. In order to obtain net-shape dimensions, the initial powder canister configuration i.e. tooling needs to be designed accurately which is a major obstacle against further development in the HIPing practice. Finite element simulation was proposed as a promising solution for the tooling design in HIPing.

Ability of finite element simulation to accurately predict the shape of HIPed component shape depends on the adopted powder compaction constitutive model. Mechanical behavior of powders in the normal HIPing cycle includes meshing micromechanical phenomena [2]. Particle re-arrangement initially by particles sliding at low pressure followed by plastic deformation of the particles and void closure at higher pressure levels. Lastly, upon holding the pressure and reaching higher temperature levels, the powder compact creeps which only account for small amount of the total deformation in the powder compact. A good constitutive model of the powder compaction should capture various behaviors of the compaction process to predict the final shape of the HIPed product accurately.

Models that are based on viscoplastic deformation or creep have been extensively used. Svoboda et al. [3] investigated the HIPing of APM2390 stainless steel powder utilizing a modified porous metal plasticity model which consider creep behavior. The results revealed very good agreement in terms of the final deformed shape compared to experimental work. Similar approach was used by Wikman et al. [4] who investigated the HIPing of APM2390 steel powder using a special model that uses either Cam – Clay model or Abouaf model based on a switching critical relative density value. The

Peer-review under responsibility of the scientific committee of the 5th CIRP Global Web Conference Research and Innovation for Future Production
doi:10.1016/j.procir.2016.07.025

results showed good agreement with experiments. Kim and Kim [5] investigated HIP of Tungsten – fiber – reinforced copper powder experimentally and numerically. Two models were compared against experimental data; namely McMeeking model [6,7] and Abouaf model [8,9]; using ABAQUS software. The comparison revealed that McMeeking model which based on micro-mechanical aspects underestimate the density distribution while Abouaf model overestimate the density distribution however both the models gave good agreement in terms of deformed shape prediction. Similar comparison had been done also before by Kim and Jeon [10] when simulating HIPing of steel 316L powder using the same two models implemented in ABAQUS subroutine called Creep and experimental data. Simulation results showed good agreement when using Abuoaf model however McMeeking model underestimated the final deformed shape and the density distribution. Baccino and Moret [11] studied HIP of 316LN steel powder using numerical modeling. Abouaf model was used to describe material viscoplastic behavior and good agreement with experimental data was achieved. Gillia et al. [12] examined simulation of HIPing of 316LN steel powder using Abouaf model to account for viscoplastic behavior. The model showed good agreement with experiments. Liu et al. [13] investigated effects of pressure on HIPing of 316L steel powder material experimentally and numerically using MSC Marc software. Perzyna viscoplastic model [14] was used and good agreement in terms of final shape was achieved. The study revealed that at high pressure of 120 MPa, the densification was the highest and most uniform compared to lower pressures. ElRakayby et al. [15] used Abouaf material model implemented through a subroutine in ABAQUS to simulate the HIPing of nickel-chromium-cobalt alloy powder. Good agreement was achieved with final deformed shape. The same material model was used by Nguyen et al. [16] to simulate Anisotropic shrinkage in HIPing of 316L steel powder using ABAQUS. A very good agreement was obtained between modeling and experiment, see figure 1. Simulation and experimental results have showed that an initially inhomogeneous relative density distribution and a temperature gradient contributes to non-uniform shrinkage of the components after HIP. Therefore, the initial relative density distribution and temperature distribution need to be implemented in the FE model for accurate results.

On the other hands, models that are based on pure plastic collapse are very attractive as they are good in shape prediction and don't need large computation time.

Lee and Kim [17] examined; the Shima–Oyane, the Fleck–Gurson, the Cam–Clay , and the modified Drucker–Prager/Cap model on Al powders cold die compaction using ABAQUS for simulation and they concluded that the Shima–Oyane model besides the proposed modified cap model agree well with experimental data of cold die compaction of AA6061 aluminum powder, see figure 2. Parteder et al. [18] studied hot forming experimentally and numerically using Abaqus/Explicit of molybdenum powder. Two constitutive models were used and compared to the experimental data namely; Gurson – Tvergard [19] model and Gologano model [20]. The latter model is a modification of Gurson model that accounts for pore shape evolution during powder compaction using an internal variable of pore shape aspect ratio. As depicted in figure 3, simulation that used Gurson – Tvergard model agreed well the experimental densification distribution when hot compressing of an already sintered (initial relative density of 95%) tapered disk at temperature of 1000 C.

Another comparison was focused on the Cam-Clay model and the modified Drucker-Prager cap model with an atomized iron-based powder [21]. The experimental data of density and tooling forces during die compaction were examined and it can be concluded that the numerical simulation with the modified Drucker-Prager cap model showed a better performance in the prediction of the density.

It have been shown that models based on pure plastic deformation as the only densification mechanism can predict the shape changes during HIPing with good accuracy [22–25] and this could be justified by the fact that 90% of the full density is gained by initially powder plastic yielding and that these models require few and easy to determine parameters. On the other hand, models that included viscoplasticity/ creep demonstrated better prediction of the densification history. However, these types of model require very large computation time and hard-to-determine parameters.

The current research focus on finite element analysis of HIPing process of steel 316L powder using three different constitutive models namely; CAM-Clay, modified Drucker-Prager and modified Drucker-Prager with creep. Comparison with experimentally deformed final geometry and densification history of the HIPed material were carried out

Nomenclature

b	Burger's vector of this material
d	Material cohesion
k	Boltzmann constant.
p	pressure
q	a measure of deviatoric stress
r	Third invariant of Cauchy stress tensor.
R	Universal gas constant.
t	time
α	A number that define transition between cap and failure surface in Drucker-Prager model
β	Angle of friction of the material
$\dot{\varepsilon}_{cr}$	The equivalent creep strain rate
σ_{eff}	Effective stress

2. Finite element model

2.1. Constitutive models

The CAM-clay plasticity model describes the inelastic behaviour of the granular material by a yield function that depends on the three stress invariants, an associated flow assumption to define the plastic strain rate, and a strain hardening theory that changes the size of the yield surface according to the inelastic volumetric strain. The model is based on the yield surface described in Equations (1-3).

$$\frac{1}{\beta^2}(\frac{p}{a}-1)^2+(\frac{q}{Ma})^2-1=0 \quad (1)$$

Where;

$$p=\frac{-trace\,[\sigma]}{3} \quad (2)$$

$$q=0.5\sigma_{eff}[1+\frac{1}{K}-(1-\frac{1}{K})(\frac{r}{\sigma_{eff}})^3] \quad (3)$$

M, β, K and *a* are constants that define the size and shape of the yield/cap surface.

Another model that frequently used to describe plasticity of granular materials is the modified Drucker-Prager model. The yield surface has two principal segments: a pressure-dependent Drucker-Prager shear failure segment and a compression cap segment. Each segment is described by a different model as below.

$$F_s=q-p\tan\beta-d=0 \quad (4)$$

$$F_c=\sqrt{[p-p_a]^2+[\frac{Rq}{1+\alpha+\alpha/\cos\beta}]^2}-R(d+p_a\tan\beta)=0 \quad (5)$$

Power law creep model, illustrated in Eq. (6), was used to describe the viscoplastic behavior of the material.

$$\bar{\dot{\varepsilon}}_{cr}=A\bar{\sigma}_{cr}^{n}t^{m} \quad (6)$$

$$Where,\ A=\frac{D_0\,b\,\exp(-\frac{Q}{RT})}{k\,T\,\sigma_0^{n-1}} \quad (7)$$

2.2. Simulation models

Steel 316 was chosen to be the powder material while the canister material to be steel 304. Steel 316 powder material particle size were ranging from 3 to 500 µm. Table 1 details the physical properties of materials that were fed to the simulation and they are based on Nguyen et al. [16] work. The properties are dependent on temperature (T) and relative density (RD).

The initial geometry of the tooling is a cylinder with internal diameter of 41.5 mm and internal height of 180 mm as depicted in Fig.1. The container/canister have a uniform thickness of 1.5 mm.

Table 1. Properties of materials used

Material property	304 stainless steel	316L stainless steel
Young's modulus (MPa)	200273-61.7T-0.039T^2	(199510-65.63T-0.0276T^2-1.754E-6T^3)RD
Poisson's ratio	0.24	0.237
Yield stress (MPa)	702.8-0.1942T-0.0003194T^2	(440-0.7173T+0.0008T^2-4.058E-7T^3)RD
Thermal conductivity (W/mm.K)	1.55E-2+1.26E-5T-9.26E-12T^2	(0.01395+1.438E-5T)RD
Specific heat (J/kg.K)	488	465.5

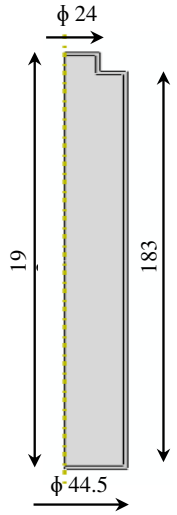

Fig. 1. Initial tooling configuration (all dimensions in mm).

Values used for the model parameters compiled from literature are detailed in Table 2. Volumetric strain hardening properties at different pressure and temperature levels were collected from literature [26]. A conventional HIP cycle was used in which temperature and pressure increase simultaneously in two hours until reaching of 1125◦C, and 110 MPa, then they are held constant for 4 hours. Afterward, temperature and pressure are decreased in one hour to room temperature and atmospheric pressure. The initial relative density was 62%.

The model was built using ABAQUS/standard 6.14 FE commercial software and the trials were run using single 2.2 GHz processor and 4 GB RAM on one node of the BlueBEAR HPC facility at University of Birmingham.

Because of tooling symmetry around its axis, the FEM model was built using axisymmetric geometry with the dimensions and geometry specified before. The temperature and pressure distribution were assumed uniform on the container surface with evolution history as specified with the HIP cycle. The model was meshed using CAX3T element (A 3-node thermally coupled axisymmetric triangle, linear

displacement and temperature) with average element size of 1.5 mm and total number of elements of 3935. Coupled-temperature-displacement analysis was utilised to account for the coupled effects of temperature, stress and strain on each other.

Table 2. Parameters of the models used for steel 316L powder.

Model	Parameters	Ref.
CAM-Clay	M=3.7, β=0.5, K=0.8	[4]
Drucker	d=3.3 MPa, β=71.5, R=0.5, ε_{vol}inl0=0.01, α=0.01, K=1	[27]
Drucker with creep	d=3.3 MPa, β=71.5, R=0.5, εvolinl0=0.01, α=0.01, K=1 power law creep parameters: n=7.5, m=0, D_0=3.7x10-5 m2/s, Q=280 kJ/mole, σ_o=1.7x10^8 Pa	[27,28]

2.3. Model validation

Validation of the model was carried out by comparison with experimentally HIPed part. Powder material were selected to be steel 316 and the canister/tooling material to be steel 304. Powder particles size were ranging from 3 to 500 µm. The initial geometry of the tooling is a cylinder with internal diameter of 41.5 mm and internal height of 180 mm as depicted in Fig. 1. The container/canister have a uniform thickness of 1.5 mm. The initial relative density were 62%. Temperature and pressure increase simultaneously in two hours until reaching of 1125◦C, and 110 MPa, then they are held constant for 4 hours. Afterward, temperature and pressure are decreased in one hour to room temperature and atmospheric pressure

3. Results and discussion

Figure 2 depicts the final deformed shape of the model using CAM-Clay, Drucker and Drucker with creep constitutive models respectively. Drucker-Prager with and without creep model results were comparable however, the CAM-clay model final deformed shape did not show much plastic compaction. The differences are due to differences in the yield surface geometry used which affect the onset of yield and subsequent material flow and volumetric hardening.

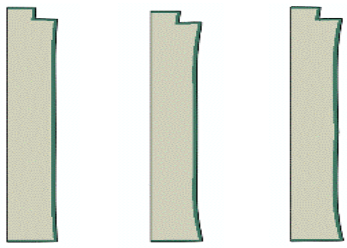

Fig.2. Final deformed shape of the CAM-Clay model (left), Drucker-Prager (middle), and Drucker with creep (right).

Figure 3 illustrates the plastic strain distribution at the end of the HIPing cycle. Average plastic strain magnitude of CAM-Clay model was 40% lower compared to Drucker-Prager model and 43% lower compared to Drucker with creep model. This indicates that the CAM-Clay model gives higher deformation resistant response than Drucker with or without creep model. The plastic strain magnitude distributions were peaking around mid-height of the workpiece and depressing at the edges (top and bottom).

Figure 4 represents the relative density distribution at the end of the HIP cycle for the three models. Similar to plastic strain magnitude, the relative density distributions were lower at the ends of the workpiece height. Similar trends were reported by Kim and Jeon [10] when HIPing of steel 316L which was attributed to the effect of friction with canister walls.

The dimensions of the experimentally HIPed component were measured at four different positions as shown in Fig. 5 and compared with simulation results of each material model. The comparison, detailed in Table 3, revealed that Drucker-Prager and Drucker with creep models predicted the final deformed dimensions of the model accurately with relative error range of 0.85-6.34% and 0.79-4.88% respectively. Predicted final deformations are contrasted in Fig. 6.

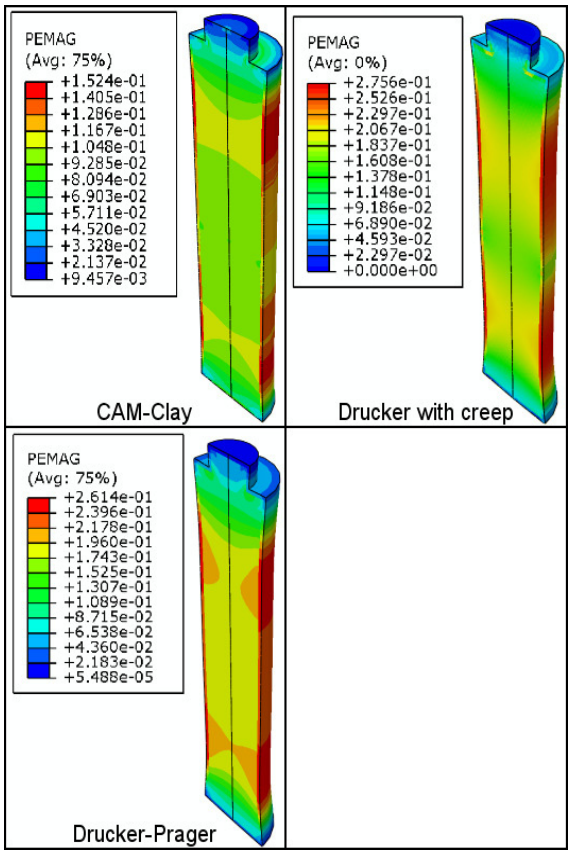

Fig. 3. Plastic strain magnitude distribution over final deformed shape of the three models.

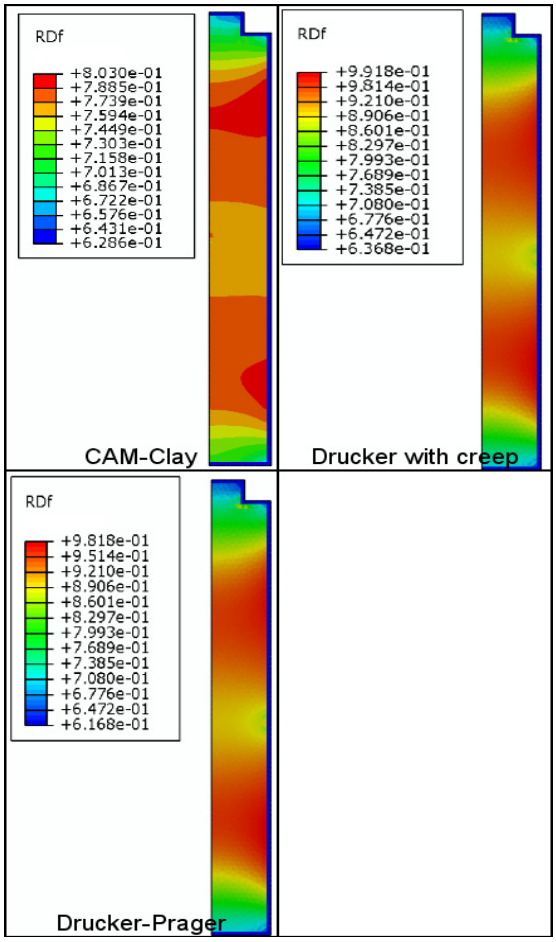

Fig. 4. Relative density distribution at the end of the HIP cycle.

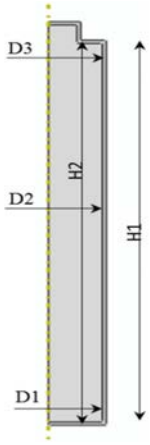

Fig. 5. Dimensions compared with experimental trials.

Table 3. Dimensional comparison of the predicted and actual deformation.

	H1	H2	D1	D2	D3
Experimental	165	163	40.8	40	41
CAM-Clay	174	173.1	42.8	41.6	43.2
Drucker-Prager	166.4	166.3	42.8	39.6	43.6
Drucker with creep	166.3	166	42.4	39.4	43

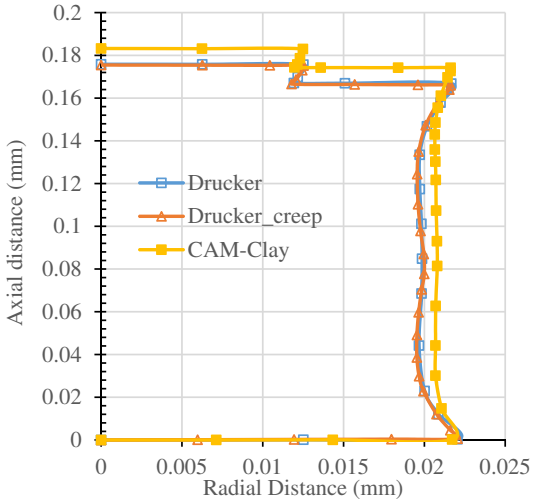

Fig. 6. Final deformed outer profile as predicted by the models.

4. Conclusions

The current investigation was focused on numerical simulation of hot isostatic pressing of steel 316L powder. A key to accurate simulation predictions is to use the suitable powder compaction constitutive model. Comparison of the simulation results with experimentally HIPed component were carried out. Relative density distribution was non-uniform with regions at the top and bottom of the canister had the lowest levels. This was attributed to the canister effects. Drucker-Prager model with creep gave the highest prediction accuracy followed by Drucker-Prager then CAM-Clay model. Final deformed shape of the HIPed component was not regular due to non-optimized initial shape and further numerical simulations will be needed for optimization.

Acknowledgment

The authors would like to acknowledge the financial support offered under the ESPRC grant (EP/M507672/1).

References

[1] Bocanegra-Bernal MH. Hot Isostatic Pressing (HIP) technology and its applications to metals and ceramics. J Mater Sci 2004;39:6399–420. doi:10.1023/B:JMSC.0000044878.11441.90.

[2] Khoei AR, Molaeinia Z, Keshavarz S. Modeling of hot isostatic

pressing of metal powder with temperature–dependent cap plasticity model. Int J Mater Form 2012;6:363–76. doi:10.1007/s12289-012-1091-x.

[3] Svoboda A, Häggblad H-Å, Karlsson L. Simulation of Hot Isostatic Pressing of a powder metal component with an internal core. Comput Methods Appl Mech Eng 1997;148:299–314. doi:10.1016/S0045-7825(96)01180-2.

[4] Wikman B, Svoboda A, Häggblad H-Å. A combined material model for numerical simulation of hot isostatic pressing. Comput Methods Appl Mech Eng 2000;189:901–13. doi:10.1016/S0045-7825(99)00406-5.

[5] Kim HG, Kim KT. Densification behavior of tungsten-fiber-reinforced copper powder compacts under hot isostatic pressing. Int J Mech Sci 2000;42:1339–56. doi:10.1016/S0020-7403(99)00060-0.

[6] Sofronis P, McMeeking RM. Creep of power-law material containing spherical voids. J Appl Mech 1992;59:S88. doi:10.1115/1.2899512.

[7] Kuhn LT, McMeeking RM. Power-law creep of powder bonded by isolated contacts. Int J Mech Sci 1992;34:563–73. doi:10.1016/0020-7403(92)90031-B.

[8] Abouaf M, Chenot JL, Raisson G, Bauduin P. Finite element simulation of hot isostatic pressing of metal powders. Int J Numer Methods Eng 1988;25:191–212. doi:10.1002/nme.1620250116.

[9] Besson J, Abouaf M. Behaviour of cylindrical HIP containers. Int J Solids Struct 1991;28:691–702.

[10] Kim K, Jeon Y. Densification behavior of 316L stainless steel powder under high temperature. Mater Sci Eng A 1998;245:64–71.

[11] Baccino R, Moret F. Numerical modeling of powder metallurgy processes. Mater Des 2000;21:359–64. doi:10.1016/S0261-3069(99)00094-1.

[12] Gillia O, Boireau B, Boudot C, Cottin A, Bucci P, Vidotto F, et al. Modelling and computer simulation for the manufacture by powder HIPing of blanket shield components for ITER. Fusion Eng Des 2007;82:2001–7. doi:10.1016/j.fusengdes.2007.03.037.

[13] Liu G, Shi Y, Wei Q, Xue P. Simulation of pressure effects on hot isostatic pressing of stainless steel powder. J Cent South Univ 2012;19:55–62. doi:10.1007/s11771-012-0972-y.

[14] Perzyna P. Fundamental Problems in Viseoplasticity. Adv Appl Mech 1966;9:243–377.

[15] ElRakayby H, Kim H, Hong S, Kim K. An investigation of densification behavior of nickel alloy powder during hot isostatic pressing. Adv Powder Technol 2015. doi:10.1016/j.apt.2015.07.005.

[16] Nguyen CV, Bezold A, Broeckmann C. ANISOTROPIC SHRINKAGE DURING HIP OF ENCAPSULATED POWDER. J Mater Process Technol 2015;226:134–45. doi:10.1016/j.jmatprotec.2015.06.037.

[17] Lee S., Kim K. Densification behavior of aluminum alloy powder under cold compaction. Int J Mech Sci 2002;44:1295–308. doi:10.1016/S0020-7403(02)00054-1.

[18] Parteder E, Riedel H, Sun D. Simulation of hot forming processes of refractory metals using porous metal plasticity models. J Refract Met Hard Mater 2002;20:287–93.

[19] Tvergaard V. Influence of voids on shear band instabilities under plane strain conditions. Int J Fract 1981;17:389–407.

[20] Gologanu M, Leblond J-B, Devaux J. Approximate models for ductile metals containing non-spherical voids—Case of axisymmetric prolate ellipsoidal cavities. J Mech Phys Solids 1993;41:1723–54. doi:10.1016/0022-5096(93)90029-F.

[21] Group PMM. Comparison of computer models representing powder compaction process: State of the art review. Powder Metall 1999;42:301–11. doi:10.1179/003258999665648.

[22] Essa K, Khan R, Hassanin H, Attallah MM, Reed R. An iterative approach of hot isostatic pressing tooling design for net-shape IN718 superalloy parts. Int J Adv Manuf Technol 2015. doi:10.1007/s00170-015-7603-3.

[23] Yuan WX, Mei J, Samarov V, Seliverstov D, Wu X. Computer modelling and tooling design for near net shaped components using hot isostatic pressing. J Mater Process Technol 2007;182:39–49. doi:10.1016/j.jmatprotec.2006.07.006.

[24] Qiu C, Adkins NJE, Hassanin H, Attallah MM, Essa K. In-situ shelling via selective laser melting: Modelling and microstructural characterisation. Mater Des 2015;87:845–53. doi:10.1016/j.matdes.2015.08.091.

[25] Hassanin H, Essa K, Qiu C, Adbelhafeez A, Adkins NJE, Attallah MM. Net-Shape Manufacturing using Hybrid Selective Laser Melting/Hot Isostatic Pressing. Rapid Prototyp J 2016;In Print.

[26] Govindarajan RM, Aravas N. Deformation processing of metal powders: Part II—Hot isostatic pressing. Int J Mech Sci 1994;36:359–72. doi:10.1016/0020-7403(94)90041-8.

[27] Wagle G. Die Compaction Simulation: Simplifying the Application of a Complex Constitutive Model Using Numerical and Physical Experiments 2006.

[28] Brown AM, Ashby MF. On the power-law creep equation. Scr Metall 1980;14:1297–302. doi:10.1016/0036-9748(80)90182-9.